Journal of Traditional and Complementary Medicine 14 (2024) 501–509

Contents lists available at ScienceDirect

Journal of Traditional and Complementary Medicine

journal homepage: www.elsevier.com/locate/jtcme

Natural 7,8-secolignans from *Schisandra sphenanthera* fruit potently inhibit SARS-CoV-2 3CL^{pro} and inflammation

Bin Li [a,1], Liansheng Qiao [b,1], Jianuo Zhang [a,1], Qi Xiao [a], Jiushi Liu [a], Bengang Zhang [a], Haitao Liu [a,*]

[a] *Key Laboratory of Bioactive Substances and Resources Utilization of Chinese Herbal Medicine, Ministry of Education, Institute of Medicinal Plant Development, Chinese Academy of Medical Sciences & Peking Union Medical College, 100193, Beijing, China*
[b] *School of Chinese Materia Medica, Beijing University of Chinese Medicine, 100029, Beijing, China*

ARTICLE INFO

Keywords:
COVID-19
SARS-CoV-2
3C-like protease
Schisandra sphenanthera fruit
UPLC-Q/TOF-MS
7,8-Secolignans
Inflammation

ABSTRACT

The coronavirus disease 2019 (COVID-19), caused by the severe acute respiratory syndrome coronavirus 2 (SARS-CoV-2), turned into a global pandemic, and there remains an urgent demand for specific/targeted drugs for the disease. The 3C-like protease (3CL^{pro}) is a promising target for developing anti-coronavirus drugs. *Schisandra sphenanthera* fruit is a well-known traditional Chinese medicine (TCM) with good antiviral activity. This study found that the ethanolic extract displayed a significant inhibitory effect against SARS-CoV-2 3CL^{pro}. Forty-four compounds were identified in this extract using ultra-performance liquid chromatography-quadrupole time-of-flight mass spectrometry (UPLC-Q-TOF/MS). Combining molecular docking and *in vitro* experiments, we found that two epimeric 7,8-secolignans, rel-(1*S*,2*R*)-1-(3,4-dimethoxyphenyl)-2-methyl-3-oxobutyl-3,4-dimethoxybenzoate (**2**) and rel-(1*S*,2*S*)-1-(3,4-dimethoxyphenyl)-2-methyl-3-oxobutyl-3,4-dimethoxybenzoate (**4**), potently inhibited 3CL^{pro} with IC_{50} values of 4.88 ± 0.60 μM and 4.75 ± 0.34 μM, respectively. Moreover, *in vivo* and *in vitro* experiments indicated that compounds **2** and **4** were potent in regulating the inflammatory response and preventing lung injury. Our findings indicate that compounds **2** and **4** may emerge as promising SARS-CoV-2 inhibitors via 3CL^{pro} inhibition and anti-inflammatory mechanisms.

1. Introduction

The coronavirus disease 19 (COVID-19) caused by the severe acute respiratory syndrome coronavirus 2 (SARS-CoV-2) has led to a devastating effect on global public health.[1] It has resulted in countless infections and caused millions of deaths worldwide.[2] Although multiple vaccines have been developed and widely administered, the continued emergence of variants of concern (VOCs) is indication of higher infectivity and immune escape.[3,4] In addition to vaccines, several existing drugs (such as Lagevrio, Paxlovid, and Remdesivir) have been approved or authorized for emergency use to help combat this disease. Nevertheless, their efficacy and safety in clinical applications are still debated.[5–7] Thus, the discovery and development of safer and more effective antiviral drugs are urgently needed.

SARS-CoV-2 is an enveloped, single-stranded RNA virus.[8] The 3C-like protease (3CL^{pro}, also called main protease or M^{pro}) is an essential protein with responsibility for the replication of the virus, which has already been identified as a crucial pharmacological target in the Middle East respiratory syndrome virus (MERS) and severe acute respiratory coronavirus syndrome (SARS-CoV).[9] This protein plays a crucial role in cleaving viral polyproteins to form essential viral proteins required for viral replication and transcription.[10] It may also interfere with the host's innate immune response[11]). Moreover, 3CL^{pro} is highly conserved among different coronaviruses and has no homologous protease in the human body, thus reducing the risk of off-target side effects.[9] Therefore, exploring 3CL^{pro} inhibitors may be an effective strategy for developing additional therapeutics against COVID-19.

Traditional Chinese medicine (TCM), which involves the use of natural products, is a good source of bioactive molecules.[12–14] TCM has been significantly effective in preventing and treating COVID-19 in China.[15–17] *Schisandra sphenanthera* (called nan-wuweizi), a well-known TCM, has long been used to treat chronic cough, kidney infections,

Peer review under responsibility of The Center for Food and Biomolecules, National Taiwan University.
* Corresponding author.
E-mail address: htliu0718@126.com (H. Liu).
[1] These authors have contributed equally to this work.

https://doi.org/10.1016/j.jtcme.2024.01.005
Received 11 March 2023; Received in revised form 10 January 2024; Accepted 10 January 2024
Available online 16 January 2024

mental problems, palpitations, spermatorrhea, and thirst.[18] Traditionally, *S. sphenanthera* is regarded as non-toxicity tonics.[18] Modern pharmacological studies have shown that the fruit of *S. sphenanthera* and its compositions possess good pharmacological effects in anti-virus, anti-inflammation, and regulating immune response.[18–21] In recent years, the antiviral activity of *S. sphenanthera* fruit has been the subject of significant research. Recently, Zhou et al. performed extensive data mining and found that *S. sphenanthera* fruit is a high-frequency Chinese herb used in the prescriptions against COVID-19.[22] Molecular docking and molecular dynamic simulation studies have suggested that it has potential value in treating SARS-CoV-2 by blocking viral replication processes.[23] In this study, we discovered that the ethanolic extract of *S. sphenanthera* fruit possesses a potential inhibitory effect on SARS-CoV-2 $3CL^{pro}$. However, to the best of our knowledge, there are no reports on the active components of *S. sphenanthera* fruit against COVID-19. Here, we aimed to characterize its chemical composition based on ultra-performance liquid chromatography-quadrupole time-of-flight mass spectrometry (UPLC-Q-TOF/MS), elucidate its anti-$3CL^{pro}$ active components, and further explore the anti-inflammatory activities of the active compounds.

2. Results

2.1. Inhibition of *S. sphenanthera* fruits extract against SARS-CoV-2 $3CL^{pro}$

A FRET-based protease assay was performed to determine the inhibitory activities of *S. sphenanthera* fruits extract against SARS-CoV-2 $3CL^{pro}$. GC376 was used as a positive control.[24] As shown in Fig. 1, the ethanolic extract exhibited 30 % and 56 % inhibition of $3CL^{pro}$ at 50 and 100 μg/mL, respectively. These results indicated that *S. sphenanthera* fruit is a potent SARS-CoV-2 $3CL^{pro}$ inhibitor. Thus, continuous chemical characterization of the ethanolic extract was performed to characterize its bioactive composition comprehensively.

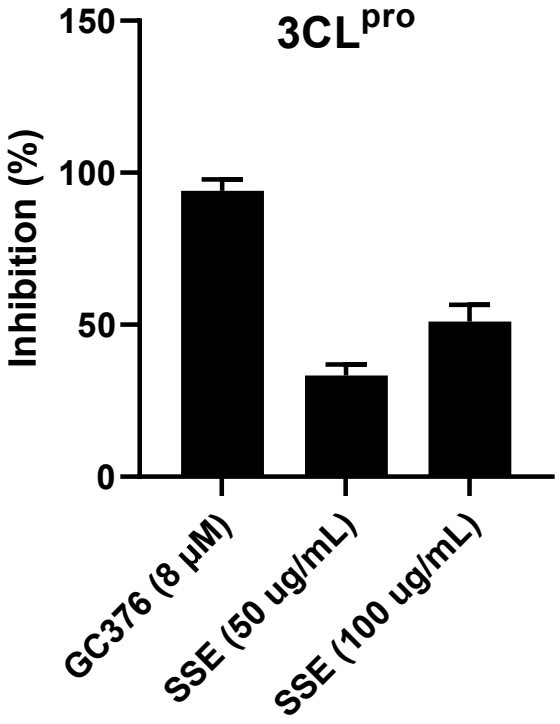

Fig. 1. Inhibition of *S. sphenanthera* fruits extract (SSE) against SARS-CoV-2 $3CL^{pro}$ *in vitro*.

2.2. Chemical characterization of the extract of *S. sphenanthera* fruits based on UPLC-Q-TOF/MS

An effective UPLC-Q-TOF/MS method was used to determine the components of the ethanolic extract. Forty-four compounds were tentatively characterized from this extract, including 40 lignans (36 dibenzocyclooctene-type, two 7,8-secolignans, one diarylbutane-type, and one 2,5-diaryltetrahydrofuran-type) and four triterpenoids (one lanostane-type and three nortriterpenoids). Among them, twenty-five compounds were further unambiguously determined by comparison with reference standards (Supplementary Figs. S1–S3). Notably, compounds **11** and **20** were identified in *S. sphenanthera* for the first time in this study. The total ion current chromatogram (TIC) of the *S. sphenanthera* fruit extract is presented in Fig. 2A, and the corresponding compound information is given in Table 1. The mass error of all the determined compounds was less than 5 ppm.

To elucidate the identification procedure of the components in this extract, compound **2**/**4** was used as a typical example. Compound **2**/**4** eluted at 3.89/3.96 min with adduct ions and fragment ions peaks at *m/z* 403.1757 $[M+H]^+$, *m/z* 425.1574 $[M+Na]^+$, *m/z* 221.1190 $[M + H–C_9H_9O_3–H_2O]^+$, *m/z* 179.1088 $[M + H–C_9H_9O_3–H_2O–C_2H_2O]^+$, and *m/z* 164.0829 $[M + H–C_9H_9O_3–H_2O–C_2H_2O–CH_3]^+$ (Fig. 2B). According to the fragmentation rules, the characteristic fragment ion at *m/z* 221.1190 $[M + H–C_9H_9O_3–H_2O]^+$ indicated that compound **2**/**4** was an oxidative cleavage of C7–C8 bond of aryltetralone lignans. The key fragment at *m/z* 179.1088 was generated by losing C_2H_2O (42 Da) from *m/z* 221.1190, which suggested the presence of an acetyl group. Additionally, a fragment ion at *m/z* 164.0829 was generated from *m/z* 179.1088, which lost a methyl group. Based on the fragmentation and retention times, compound **2**/**4** was tentatively identified as rel-(1*S*,2*R*)-1-(3,4-dimethoxyphenyl)-2-methyl-3-oxobutyl-3,4-dimethoxybenzoate or rel-(1*S*,2*S*)-1-(3,4-dimethoxyphenyl)-2-methyl-3-oxobutyl-3,4-dimethoxybenzoate.

2.3. Screening of the active compounds against $3CL^{pro}$ based on molecular docking

To explore the active compounds against $3CL^{pro}$, molecular docking studies were performed on the 44 compounds using CDOCKER. The initial ligand (baicalein) was utilized to determine the active site with a radius of 8.00 Å, and the RMSD values among re-docked baicalein and crystal structures were 0.29 Å. A water molecule remains in the active pocket, which may play a positive role in forming a hydrogen bond. Re-docking results indicated that the docking model was appropriate. The key binding sites were HIS41, CYS44, MET49, ASN142, GLY143, SER144, CYS145, MET165, GLU166, and water, which were consistent with previous reports.[25]

As shown in Fig. 3 and Supplementary Table S1, compounds **2** and **4** showed high binding affinities with SARS-CoV-2 $3CL^{pro}$ (CDOCKER energy = −29.75 and −28.48 kcal/mol, respectively), suggesting that **2** and **4** have potential $3CL^{pro}$ inhibitory effects. Compounds **2** and **4** showed similar binding modes and key residues, including THR26, CYS145, MET49, and ASP187. Based on the comparison of binding modes of baicalein, compounds **2** and **4**, CYS145, and MET49 were the key residues of $3CL^{pro}$ inhibitors (Fig. S4).

2.4. Verification of the inhibitory effects of compounds **2** and **4** on $3CL^{pro}$ *In vitro*

Using UPLC-Q-TOF/MS analysis, compounds **2** (95 mg) and **4** (115 mg) were obtained via chromatographic separation and purification. The structures of **2** and **4** were confirmed by HRESIMS and NMR data analyses (Supplementary Figs. S5–S8). Inhibitory activities were then evaluated using enzymatic assays. At 8 μM, compounds **2** and **4**

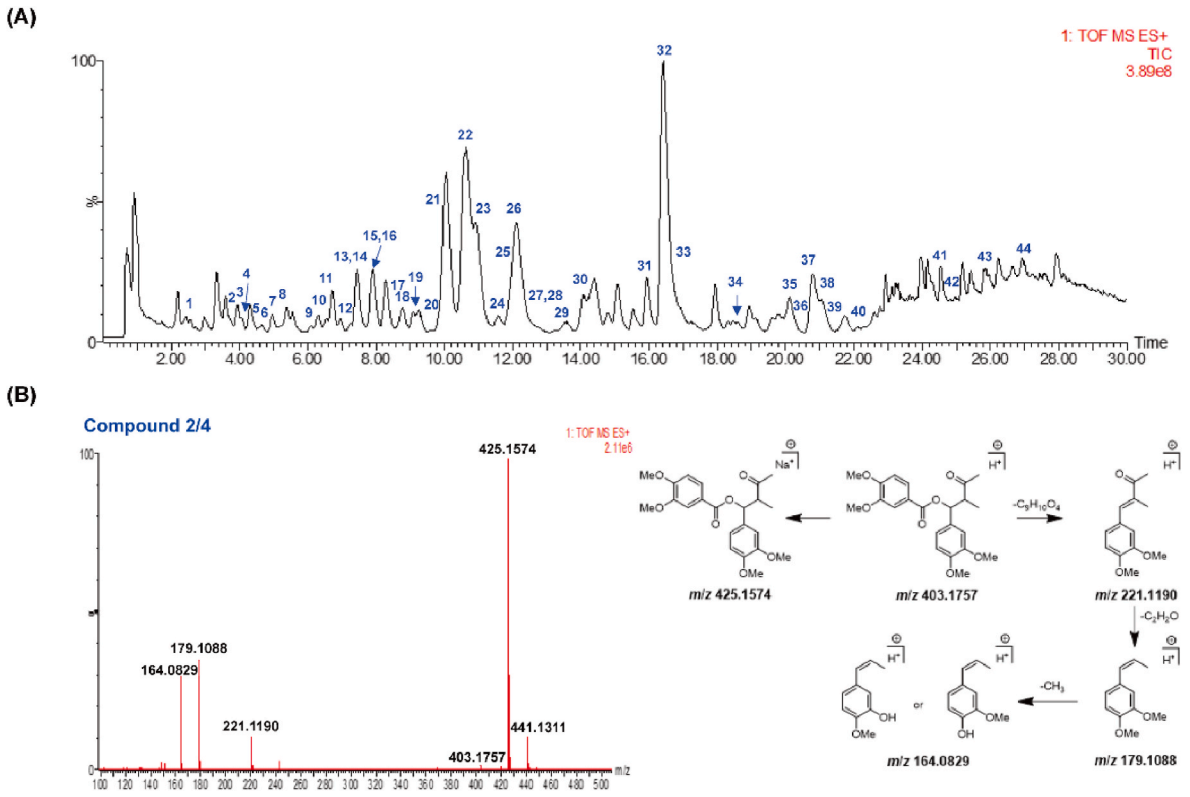

Fig. 2. The total ion chromatogram (TIC) of the ethanol extract of *S. sphenanthera* fruits (A), and the MS spectra as well as possible fragmentation pathways of compound **2**/**4** (B) in positive ion mode.

exhibited inhibition rates of 55.13 % and 52.78 %, respectively, with 80.34 % inhibition for the positive control (GC376). As shown in Fig. 4, the IC_{50} values of compounds **2** and **4** detected were 4.88 ± 0.60 μM and 4.75 ± 0.34 μM, respectively. Overall, compounds **2** and **4** showed definite SARS-CoV-2 $3CL^{pro}$ inhibitory activities.

2.5. Anti-inflammatory activities of compounds 2 and 4 in ALI mice model

To further evaluate the anti-inflammatory activity of compounds **2** and **4,** an LPS-induced ALI mouse model was established. Histopathological changes in the lungs were observed using haematoxylin and eosin (H&E) staining. As shown in Fig. 5, the alveolar epithelial structures were intact, the morphology of alveoli was uniform, and there were no inflammatory cells infiltration in the trachea and bronchi in the control group. In contrast, there were no significant difference between a single administration of **2**/**4** and CMC-Na. After LPS stimulation in mice, remarkable inflammatory cell infiltration into the alveoli and alveolar septum, alveolar wall thickening, edema, and congestion, indicated that the modeling of lung injury was successful. Notably, treatment with compounds **2** and **4** (20 mg/kg) significantly attenuated these histopathological changes.

Furthermore, the levels of the pro-inflammatory cytokines IL-6, TNF-α, IL-8, and IL-1β in BALF were determined. Consistent with the histopathological improvement, no significant differences were observed in the BALF IL-6, TNF-α, IL-8, and IL-1β levels of mice between compound **2**/**4** group and control group, suggesting that compounds **2** and **4** are safe for normal mice at this dose (Fig. 6). In contrast, these inflammatory factors in BALF were significantly increased in the model group, compared with the control group. However, compounds **2** and **4** (20 mg/kg) treatment effectively reduced the levels of IL-6, TNF-α, IL-8, and IL-1β in the BALF. These results suggest that compounds **2** and **4** possess significant anti-inflammatory effects and can down-regulate the expression of inflammatory cytokines.

2.6. Anti-inflammatory activities of compounds 2 and 4 in LPS-induced RAW 264.7 cells

Here, we further used an LPS-induced RAW 264.7 cells model to study the anti-inflammatory effects of compounds **2** and **4** *in vitro*. We initially assessed the cytotoxicity of compounds **2** and **4** using a CCK8 assay. The results showed that compounds **2** and **4** had no cytotoxic effect on RAW 264.7 cells at concentrations below 50 μM (Fig. 7A). Thus, we decided to use concentrations below 50 μM in further experiments. As shown in Fig. 7B, LPS stimulation dramatically increased nitric oxide (NO) production. Treatment with compound **4** (25 and 50 μM) significantly decreased NO production in a dose-dependent manner. By contrast, compound **2** reduced the NO production at 50 μM.

3. Discussion

TCM is a promising resource for developing novel anti-SARS-CoV-2 drugs based on its safety and efficacy in COVID-19 treatment.[26] Natural molecules isolated from TCM have been reported to exhibit remarkable inhibitory activity against SARS-CoV-2 and other coronaviruses.[8,27] *S. sphenanthera* fruit, a well-known TCM, has high health value and biological activity. Extensive studies have shown that *S. sphenanthera* fruit and its components exhibit antiviral activities against the human immunodeficiency virus, human alphaherpesvirus 2, and adenovirus.[19–21] In this study, we found that the ethanol extract of *S. sphenanthera* fruit showed good inhibitory activity against SARS-CoV-2 $3CL^{pro}$. These results suggest that *S. sphenanthera* fruit could be a practical source to identify $3CL^{pro}$ inhibitors. UPLC-Q-TOF/MS is a powerful analytical method for analysing the chemical components of TCM.[28] Forty-four compounds were identified in this extract by UPLC-Q-TOF/MS, including 40 lignans (36 dibenzocyclooctene-type, one diarylbutane-type, one 2,5-diaryltetrahydrofuran-type, and two 7, 8-secolignans) and four triterpenoids (one lanostane-type and three nortriterpenoids). Among these, compounds **11** and **20** were identified

Table 1
44 compounds identified and characterized in *S. sphenanthera* fruits extract by using UPLC-Q-TOF/MS.

No.	t_R (min)	Compounds	Molecular formula	Adduct	Extraction mass (Da)	Error (ppm)
1	2.34	gomisin H[a]	$C_{23}H_{30}O_7$	$[M+H]^+$	419.2077	1.7
2	3.89	rel-(1*S*,2*R*)-1-(3,4-dimethoxyphenyl)-2-methyl-3-oxobutyl-3,4-dimethoxybenzoate	$C_{22}H_{26}O_7$	$[M+Na]^+$	425.1574	−0.5
3	3.94	schisandrol A[a]	$C_{24}H_{32}O_7$	$[M+H]^+$	433.2221	−1.2
4	3.96	rel-(1*S*,2*S*)-1-(3,4-dimethoxyphenyl)-2-methyl-3-oxobutyl-3,4-dimethoxybenzoate	$C_{22}H_{26}O_7$	$[M+Na]^+$	425.1574	−0.5
5	4.34	schisantherin E[a]	$C_{30}H_{34}O_9$	$[M+NH_4]^+$	556.2541	−1.1
6	4.66	gomisin D[a]	$C_{28}H_{34}O_{10}$	$[M+H]^+$	531.2233	0.6
7	4.98	gomisin J[a]	$C_{22}H_{28}O_6$	$[M+H]^+$	389.1977	3.3
8	5.19	schisandrol B[a]	$C_{23}H_{28}O_7$	$[M+Na]^+$	439.1744	2.5
9	6.35	gomisin E	$C_{28}H_{34}O_9$	$[M+H]^+$	515.2277	−0.8
10	6.54	tigloylgomisin H	$C_{28}H_{36}O_8$	$[M+H]^+$	501.2475	−2.6
11	6.85	arisanschinin G	$C_{22}H_{28}O_6$	$[M+H]^+$	389.1977	3.3
12	7.11	angeloylgomisin H	$C_{28}H_{36}O_8$	$[M+H]^+$	501.2477	−2.2
13	7.25	angeloylgomisin Q	$C_{29}H_{38}O_9$	$[M+NH_4]^+$	548.2871	2.0
14	7.69	benzoylgomisin H	$C_{30}H_{34}O_8$	$[M+H]^+$	523.2324	−1.5
15	7.80	tigloylgomisin Q	$C_{29}H_{38}O_9$	$[M+NH_4]^+$	548.2874	2.6
16	7.89	gomisin O[a]	$C_{23}H_{28}O_7$	$[M+Na]^+$	439.1744	2.5
17	8.58	chicanine[a]	$C_{20}H_{22}O_5$	$[M+H]^+$	343.1554	2.6
18	8.79	gomisin G[a]	$C_{30}H_{32}O_9$	$[M+NH_4]^+$	554.2389	−0.2
19	9.22	(7*S*,8*S*,*R*-biar)-6,6,7,8-tetrahydro-12,13-methylenedioxy-1,2,3,14-tetramethoxy-7,8-dimethyldibenzo[*a*,*c*]cyclooocten-9-one[a]	$C_{23}H_{26}O_7$	$[M+H]^+$	415.1750	−1.7
20	9.68	(−)-Gomisin K_1[a]	$C_{23}H_{30}O_6$	$[M+H]^+$	403.2104	−4.2
21	10.05	(+)-Gomisin K_2[a]	$C_{23}H_{30}O_6$	$[M+H]^+$	403.2114	−1.7
22	10.64	schisantherin A[a]	$C_{30}H_{32}O_9$	$[M+NH_4]^+$	554.2389	−0.2
23	10.96	schisantherin B[a]	$C_{28}H_{34}O_9$	$[M+NH_4]^+$	532.2565	3.4
24	11.35	tigloylgomisin P	$C_{28}H_{34}O_9$	$[M+NH_4]^+$	532.2565	3.4
25	11.67	schisantherin D[a]	$C_{29}H_{28}O_9$	$[M+NH_4]^+$	538.2063	−2.6
26	12.12	schsanhenol[a]	$C_{23}H_{30}O_6$	$[M+H]^+$	403.2104	−4.2
27	12.65	(+)-Gomisin M_1	$C_{22}H_{26}O_6$	$[M+H]^+$	387.1821	3.3
28	12.65	(+)-Gomisin M_2[a]	$C_{22}H_{26}O_6$	$[M+H]^+$	387.1821	3.3
29	13.53	methylgomisin R	$C_{23}H_{26}O_7$	$[M+H]^+$	415.1750	−1.7
30	13.99	schisantherin C	$C_{28}H_{34}O_9$	$[M+H]^+$	515.2277	−0.8
31	15.92	anwuligan[a]	$C_{20}H_{24}O_4$	$[M+H]^+$	329.1750	−0.9
32	16.43	d-epigalbacin[a]	$C_{20}H_{20}O_5$	$[M+H]^+$	341.1382	−2.1
33	16.47	schisandrin A[a]	$C_{24}H_{32}O_6$	$[M+H]^+$	417.2293	3.8
34	18.58	schisandrin B[a]	$C_{23}H_{28}O_6$	$[M+H]^+$	401.1958	−1.5
35	20.14	benzoylisogomisin O	$C_{30}H_{32}O_8$	$[M+H]^+$	521.2172	−0.6
36	20.21	angeloylisogomisin O	$C_{28}H_{34}O_8$	$[M+Na]^+$	521.2172	4.0
37	20.78	schisandrin C[a]	$C_{22}H_{24}O_6$	$[M+H]^+$	385.1638	−3.4
38	20.80	benzoylgomisin O[a]	$C_{30}H_{32}O_8$	$[M+Na]^+$	543.2017	4.1
39	20.93	angeloylgomisin O[a]	$C_{28}H_{34}O_8$	$[M+Na]^+$	521.2172	4.0
40	21.62	interiotherin A[a]	$C_{29}H_{28}O_8$	$[M+Na]^+$	527.1662	−3.8
41	24.29	nigranoic acid	$C_{30}H_{46}O_4$	$[M+H]^+$	471.3470	−0.8
42	24.59	kadsuric acid	$C_{30}H_{46}O_4$	$[M+H]^+$	471.3470	−0.8
43	25.95	ganwuweizic acid	$C_{30}H_{46}O_3$	$[M+H]^+$	455.3521	−0.9
44	26.96	kadsuric acid 3-methylester	$C_{31}H_{48}O_4$	$[M+H]^+$	485.3617	−2.9

[a] Identified with reference compounds accurately, and the others were tentatively assigned by literature data.

in *S. sphenanthera* for the first time.

It is well known that computerized screening combined with experimental validation is an effective method for screening potential pharmacological components from many compounds.[29] Compared with traditional screening, merged analysis is easy, time-saving, and low-cost.[30] In this study, virtual screening and FRET were used to screen for effective components of $3CL^{pro}$. With the help of molecular docking studies and *in vitro* experiments, we found that two 7,8-secolignans, **2** and **4** exhibited potent antiviral activity against SARS-CoV-2 $3CL^{pro}$.

Furthermore, a hallmark of COVID-19 is a lung inflammation characterised by excessive inflammatory cell infiltration and the overproduction of pro-inflammatory cytokines such as IL-6, IL-8, TNF-α, and IL-1β, which is known as "cytokine storm".[31] This cytokine storm can lead to pulmonary fibrosis consolidation, acute respiratory distress syndrome, multiple organ failure, and death.[32] Studies have shown that anti-inflammatory therapies that modulate pro-inflammatory cytokines (such as IL-6 and IL-8) against COVID-19 are significantly effective.[33–35] Schisandrae lignans are well known for their anti-inflammatory activities.[18] Thus, we further investigated the anti-inflammatory efficacy of compounds **2** and **4** in an LPS-induced ALI mouse model. Histopathological results showed that oral compounds **2** and **4** significantly reduced inflammatory cell infiltration and airspace enlargement in the lung tissues. Meanwhile, compounds **2** and **4** treatment remarkably reduced the levels of the pro-inflammatory cytokines IL-6, IL-8, TNF-α, and IL-1β in BALF.

Macrophages play a key role in the pathogenesis of SARS-CoV-2 infection-related inflammatory response.[36] Thus, we further used a classical macrophage model of LPS-induced RAW 264.7 cells to study the anti-inflammatory effects of compounds **2** and **4** *in vitro*. The results showed that treatment with compounds **2** and **4** significantly inhibited

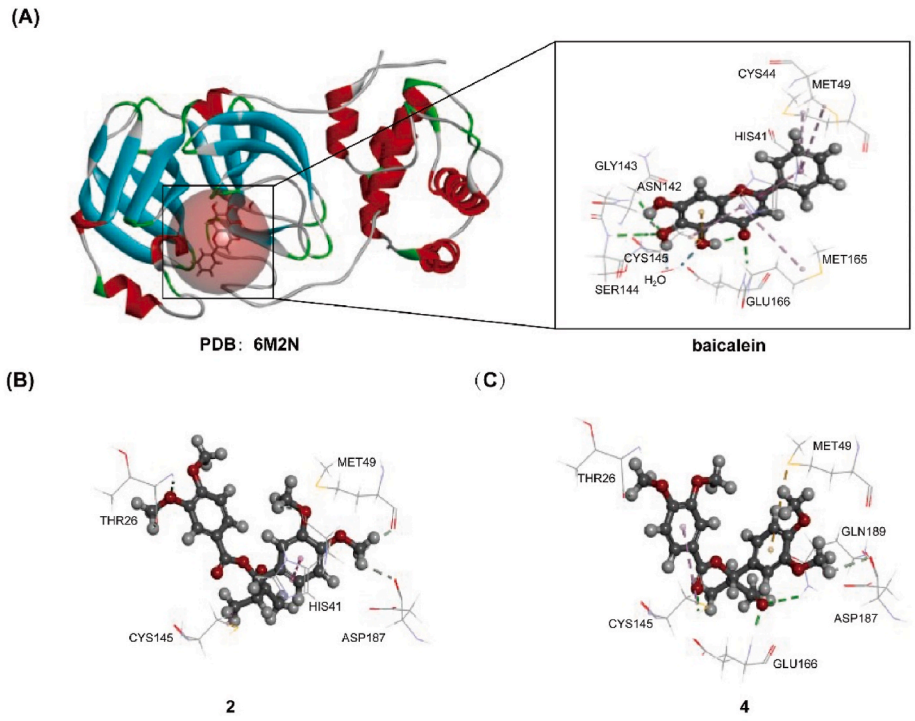

Fig. 3. Binding modes of compounds **2** and **4** with $3CL^{pro}$ by CDOCKER analysis. (A) The crystal structure of $3CL^{pro}$ (6M2N) and the binding mode of the initial ligand (baicalein). (B) Binding mode of compound **2** with $3CL^{pro}$. (C) Binding mode of compound **4** with $3CL^{pro}$.

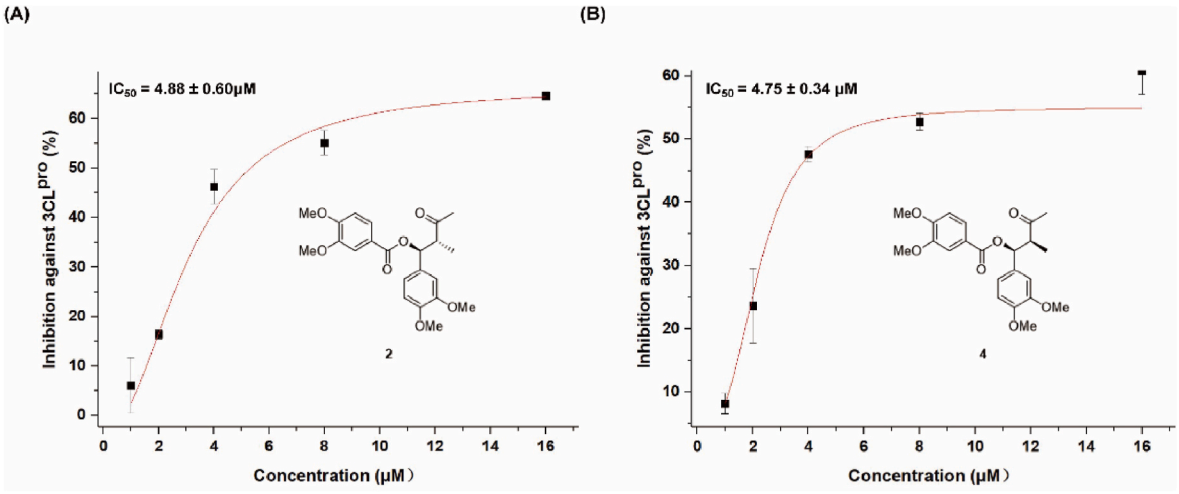

Fig. 4. The inhibitory activities of compounds **2** (A) and **4** (B) against SARS-CoV-2 $3CL^{pro}$.

NO production in LPS-induced RAW 264.7 cells. Considered together, these findings indicate that compounds **2** and **4** not only inhibit SARS-CoV-2 $3CL^{pro}$ but also regulate hyper-inflammatory responses and prevent lung injury, thus suggesting that they might be good candidates for the prevention and treatment of COVID-19. Admittedly, our study is only based on enzymatic assays at a protein level, not real anti-viral assays. Although the anti-$3CL^{pro}$ active compounds **2** and **4** were identified and further explored for their anti-inflammatory activities, whether they could inhibit SARS-CoV-2 replication still need to be confirmed by a cell-based assay.

In conclusion, in this study, we demonstrate that the ethanol extract of *S. sphenanthera* fruit is effective in inhibiting SARS-CoV-2 $3CL^{pro}$. Forty-four components were identified in this extract by UPLC-Q-TOF/MS. Molecular docking and experiments confirmed that its inhibitory activities against $3CL^{pro}$ was attributable to compounds **2** and **4** contained in this extract. Notably, compounds **2** and **4** also exhibit good anti-inflammatory and protective effects against lung injury. Our study provides insight into the natural metabolites from *S. sphenanthera* fruit with therapeutic potential for treating COVID-19.

4. Materials and methods

4.1. Materials and Reagents

MS-grade methanol (MeOH) and acetonitrile (MeCN) were provided by Thermo Fisher Scientific Co., Ltd. (Shanghai, China). Ultra-pure water was collected using a Milli-Q ultrapure water system (Milford, USA). Analytical grade petroleum ether, ethyl acetate (EtOAc), EtOH, and MeOH were procured from Beijing Chemical Reagent Co. Ltd. (Shanghai, China). The SARS-CoV-2 $3CL^{pro}$ was purchased from

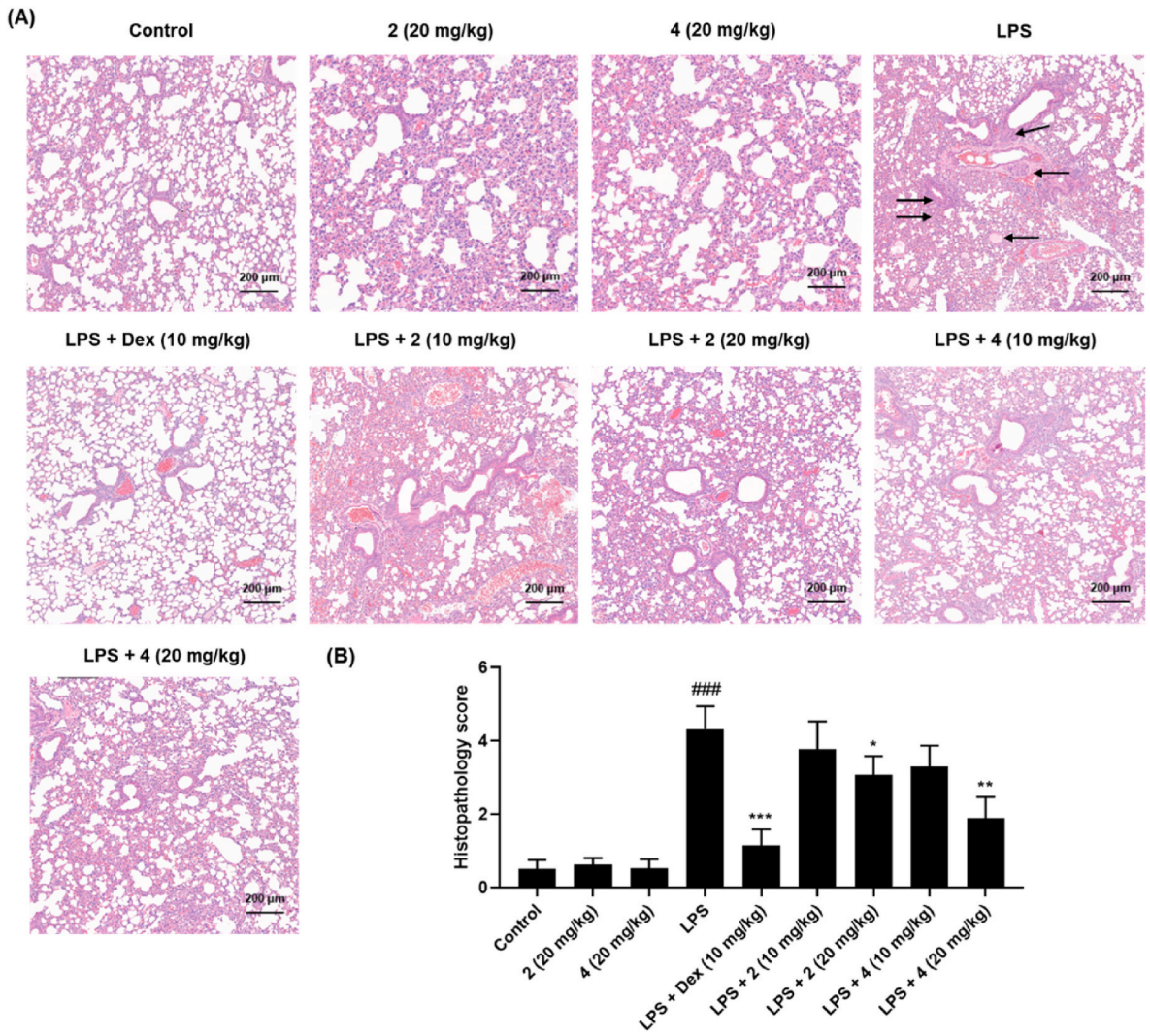

Fig. 5. Effect of compounds **2** and **4** on the histopathological changes in lung tissues in normal and LPS-induced ALI mice. (A) The images of representative haematoxylin and eosin (H&E)-stained lung sections. (B) Pathology evaluation for the therapeutic effect of compounds **2** and **4**. $^{###}P < 0.01$ *vs*. control group, $^{*}P < 0.05$, $^{**}P < 0.01$, $^{***}P < 0.001$ *vs*. model group.

Novoprotein Technology Co., Ltd. Lipopolysaccharide (LPS) was obtained from Sigma-Aldrich (St. Louis, MO, USA). Dexamethasone (Dex) was supplied by Shanghai Yuanye Biotechnology Co., Ltd. (Shanghai, China). The interleukin (IL)-6 and tumour necrosis factor (TNF)-α kits were obtained from BioLegend (San Diego, USA). The IL-1β kit was purchased from Thermo Fisher Scientific (Waltham, MA). IL-8 and NO kits were obtained from Neobioscience (Shenzhen, China) and Beyotime (Shanghai, China), respectively.

4.2. Preparation of S. sphenanthera fruits extract

The fruits of *S. sphenanthera* were collected from Hanzhong (Shanxi, China). Dried fruits of *S. sphenanthera* (5 kg) were powdered and extracted with 95 %, 80 %, and 65 % aqueous ethanol (each at a 10-fold volume). All supernatants were mixed and concentrated under reduced pressure to obtain the *S. sphenanthera* ethanolic extract.

4.3. SARS-CoV-2 $3CL^{Pro}$ inhibition assay

A fluorescence resonance energy transfer (FRET) method was used to assess the inhibitory activity of the extracts or compounds against the SARS-CoV-2 $3CL^{pro}$ by fluorogenic substrate Dabcyl-KTSAVLQSGFRKME-Edans.[3] Briefly, a final concentration of 12.5 μg/mL $3CL^{pro}$ was mixed with 3 mM substrate, 50–100 μg/mL extract or 1–16 μM compound in 100 μL assay buffer (20 mM Tris-HCl, pH 7.0) at 25 °C for 10 min. GC376 was used as a positive control. The fluorescent signals at an emission wavelength of 535 nm and excitation wavelength of 340 nm were continuously measured using a FlexStation 3 Multi-Mode Microplate Reader. The enzyme activity was calculated according to the following logistic derivative equation:

$$\mathbf{A} = ((\Delta \boldsymbol{OD}_{test})\boldsymbol{df}) \,/\, (\Delta \boldsymbol{OD}_{Control}(\mathbf{2.204092} \times \boldsymbol{C} \times \boldsymbol{V}_s))$$

A, enzyme activity; df, dilution factor; OD, absorption change/min; Vs, sample volume; C, concentration of $3CL^{pro}$.

4.4. UPLC-Q-TOF/MS analyze

UPLC-Q-TOF/MS analysis was performed on a Waters Acquity UPLC system equipped with a Waters mass spectrometer (Xevo G2-XS TOF, Waters, Milford, MA, USA). The ethanol extract (10 mg) was dissolved in 10 mL of methanol, and then was filtered through a 0.22 μm filter. Chromatographic separation was performed on an ACQUITY BEH C_{18} column (2.1 × 100 mm I.D., 1.7 mm, Waters Corporation, Milford, MA, USA) at a 0.3 mL/min flow rate. The mobile phase comprised 0.1 % formic acid in water (solvent A) and acetonitrile (solvent B). The column

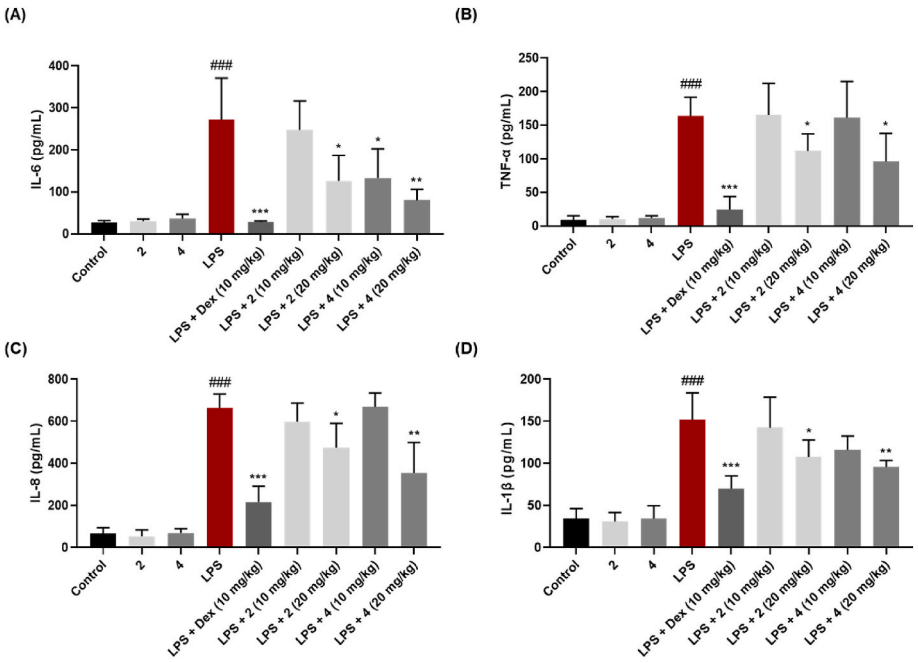

Fig. 6. Effect of compounds **2** and **4** on IL-6 (A), TNF-α (B), IL-8 (C), and IL-1β (D) production in BALF. The data are the mean ± SD (n = 5). $^{###}P < 0.01$ *vs.* control group, $^{*}P < 0.05$, $^{**}P < 0.01$, $^{***}P < 0.01$ *vs.* model group.

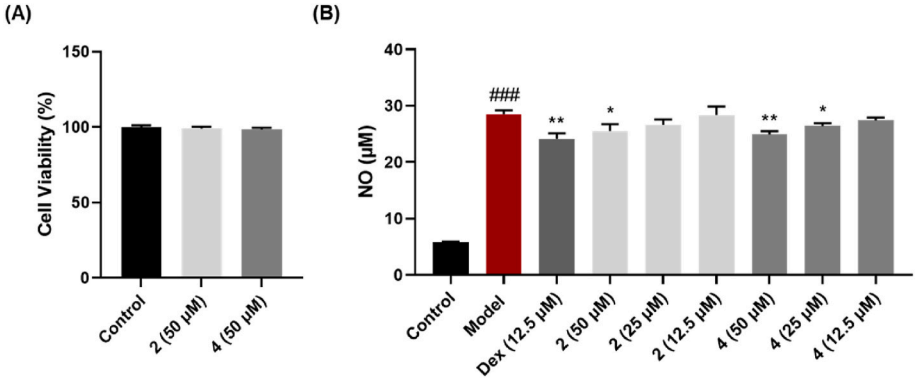

Fig. 7. Effect of compounds **2** and **4** on NO production in LPS-induced RAW 264.7 cells. (A) Cytotoxic activity of compounds **2** and **4** against RAW 264.7 cells at a concentration of 50 μM. (B) Level of NO treated with compounds **2** and **4** (12.5, 25, and 50 μM) in LPS-induced RAW 264.7 cells. The data are the mean ± SD (n = 3). $^{##}P < 0.01$ *vs.* control group, $^{*}P < 0.05$, $^{**}P < 0.01$ *vs.* model group.

temperature and injection volume were set at 30 °C and 3 μL, respectively. A linear gradient was set as follows: 0–4 min, 42–45 % B; 4–6 min, 45–48 % B; 6–12 min, 48 % B; 12–16 min, 48–62 % B; 16–21 min, 62 % B; 21–22 min, 62–85 % B; 22–29 min, 85–95 % B; 29–30 min, 95 % B.

A mass spectrometer equipped with an ESI source was operated in the positive ionisation mode. The scanning mass-to-charge ratio was set between *m/z* 50 and 1200 Da. The MS conditions were as follows: capillary voltage, 3 kV; source temperature, 100 °C; desolvation temperature, 350 °C; cone gas flow, 50 L/h; desolvation gas flow, 600 L/h. N_2 was used as the auxiliary and nebulizer gas. Mass accuracy was calibrated using the Leu-Enkephalin ions at *m/z* 556.2771 and 554.2615. Data analysis was performed using Waters MassLynx 4.2 software (Waters).

4.5. Virtual screening

Based on the UPLC-Q-TOF/MS-determined ingredients from the ethanolic extract of *S. sphenanthera* fruits, molecular docking was performed to screen the inhibitors of $3CL^{pro}$. The 3D conformations of the identified compounds were generated using Discovery Studio (Accelrys Inc., San Diego, CA, USA) and minimized in the CHARMm force field with MMFF94 partial charge. The crystal structure of $3CL^{pro}$ was downloaded from the Protein Data Bank (PDB, ID: 6M2N) database.[25] The active binding site of $3CL^{pro}$ was determined using the initial ligand (baicalein). Before the docking study, crystallographic waters (out of the active binding site) were removed from the complex, and hydrogen atoms were added. CDOCKER algorithms were used for molecular docking. The initial ligand was extracted from the active binding site and re-docked into the site to calculate root-mean-square deviation (RMSD). RMSD less than 2.00 Å indicated that the docking model was appropriate and could reproduce the binding mode of the receptor and ligand. The docking score, key residues, and binding poses were utilized to analyze the interaction between $3CL^{pro}$ and the active compounds from *S. sphenanthera* fruit.

4.6. Chromatographic Isolation and purification

The ethanolic extract of *S. sphenanthera* fruits (1.5 kg) was chromatographed on a silica gel column (22 × 50 cm, 8 kg, 100–200 mesh, Qingdao Marine Chemical Inc. Ltd.) and eluted with petroleum ether-EtOAc (1:0–0:1, v/v) to obtain seven fractions A-G. Fraction G (420 g) was separated on a silica gel column (200–300 mesh) and eluted with a gradient of ether-EtOAc (6:1–0:1, v/v) to obtain subfractions GA, GB, GC, and GD. Subfraction GB (35 g) was purified over a Zorbax C_{18} semi-preparative column (9.4 × 250 mm, 5 μm; MeCN–H_2O, 25:75, v/v) to obtain **2** and **4**.

4.7. Anti-inflammatory assay on LPS induced ALI mouse model

Male BALB/c mice (18–22 g, SPF) were purchased from Beijing Vital River Laboratory Animal Technology Co., Ltd. (Beijing, China). Animals were kept in a temperature- and humidity-controlled room under a 12 h light/dark cycle. All the mice had *ad libitum* access to food and water. All animal experimental procedures were performed in accordance with the Guidelines for the Care and Use of Laboratory Animals (National Institutes of Health) and approved by the Experimental Animal Ethical Committee of the Institute of Medicinal Plant Development, Chinese Academy of Medical Sciences.

108 mice were randomly divided into nine groups (n = 12): control, compound **2** (20 mg/kg), compound **4** (20 mg/kg), LPS, LPS + dexamethasone (Dex), LPS + compound **2** (10 mg/kg), LPS + compound **2** (20 mg/kg), LPS + compound **4** (10 mg/kg), LPS + compound **4** (20 mg/kg) groups. An ALI mouse model was established by intranasal administration of LPS at a dose 3 mg/kg. Mice in the treatment groups were orally administered compound **2** (10 mg/kg and 20 mg/kg), compound **4** (10 mg/kg and 20 mg/kg), and Dex (10 mg/kg), followed by LPS stimulation. The control group was administered an equal volume of 0.5 % CMC-Na solution. After 8 h, the mice were anaesthetised with an overdose of pentobarbital (50 mg/kg).

4.7.1. Histological evaluation

Lung tissues were collected and fixed in 4 % paraformaldehyde. According to our previously reported method, H&E staining and histological scoring were performed to assess the infiltration of inflammatory cells into the lung tissues.[28]

4.7.2. Bronchoalveolar Lavage Fluid (BALF) Collection and cytokine Enzyme-Linked Immunosorbent Assay (ELISA)

After exsanguination, the lungs were washed three times by intratracheal instillation using 0.6 mL ice-cold PBS to obtain the BALF. The BALF was further centrifuged (400×*g*) immediately for 10 min at 4 °C and the supernatant was collected. The levels of IL-6, IL-8, IL-1β, and TNF-α in BALF were detected using commercial ELISA assay kits.

4.8. Anti-inflammatory assay in LPS-Stimulated RAW 264.7 cells

4.8.1. Cell culture and viability

RAW 264.7 cells were cultured and maintained in Dulbecco's modified Eagle medium (DMEM, Thermo Fisher Scientific) at 37 °C in a 5 % CO_2 humidified atmosphere. Cells were seeded in 96-well plates at 2×10^4 cells/well and incubated for 24 h. The samples were then treated for 24 h. Cell viability was measured in the CCK8 assay according to the manufacturer's protocol.[28] All experiments were performed in triplicate.

4.8.2. Measurement of nitric oxide (NO) production

RAW 264.7 cells (2×10^4 cells/well) were seeded in 96-well plates for 5 h, and then treated with the sample or Dex for 1 h before LPS stimulation. LPS was subsequently added at 1 μg/mL concentration for 24 h. The NO levels in the supernatant were determined using a commercial kit following the manufacturer's instructions. All experiments were performed in triplicate.

4.9. Statistical analyses

The results are expressed as mean ± standard deviation (SD). Statistical analyses were performed using one-way analysis of variance (ANOVA), and statistically significant was set at $P < 0.05$.

Author contributions

Conceptualization, H.T.L. and B.L.; methodology, B.L. and L.S.Q.; software, L.S.Q. and J.S.L.; validation, B.L., L.S.Q., Q.X. J.S.L. and J.N.Z.; formal analysis, Q.X.; investigation, B.L., L.S.Q. and J.N.Z.; data curation, Q.X.; writing—original draft preparation, B.L., L.S.Q. and J.N.Z.; writing—review and editing, B.G.Z. and H.T.L.; visualization, J.S.L.; supervision, B.G.Z.; project administration, B.G.Z.; funding acquisition, H.T.L. and B.L. All authors have read and agreed to the published version of the manuscript."

Funding

This work was supported by the Beijing Natural Science Foundation (No. 82304708); the National Natural Science Foundation of China (No. 82304708); the CAMS Innovation Fund for Medical Sciences (2023-I2M-QJ-013, 2021-I2M-1–031, and 2022-I2M-2-002).

Institutional review board statement

Not applicable.

Informed consent statement

Not applicable.

Conflicts of interest

The authors declare that they have no known competing financial interests or personal relationships that could have appeared to influence the work reported in this paper.

Declaration of competing interest

The authors declare no conflict of interest.

Appendix A. Supplementary data

Supplementary data to this article can be found online at https://doi.org/10.1016/j.jtcme.2024.01.005.

List of abbreviations

COVID-19 The coronavirus disease 2019
SARS-CoV-2 syndrome coronavirus 2
3CL^{pro} the 3C-like protease
TCM traditional Chinese medicine;
UPLC-Q-TOF/MS ultra-performance liquid chromatography-quadrupole time-of-flight mass spectrometry
MERS middle East respiratory syndrome virus
VOCs variants of concern
SARS-CoV severe acute respiratory coronavirus syndrome
SSE *S. sphenanthera* fruits extract
TIC the total ion current chromatogram
H&E haematoxylin and eosin
MeOH methanol
MeCN acetonitrile;
EtOAc ethyl acetate
LPS Lipopolysaccharide;
Dex dexamethasone

IL	interleukin
TNF	tumour necrosis factor
FRET	fluorescence resonance energy transfer
RMSD	root-mean-square deviation
ELISA	enzyme-linked immunosorbent assay
BALF	bronchoalveolar lavage fluid
DMEM	Dulbecco's modified Eagle medium
NO	nitric oxide;
SD	standard deviation
ANOVA	one-way analysis of variance

References

1. Gorbalenya AE, Baker SC, Baric RS, et al. The species severe acute respiratory syndrome-related coronavirus: classifying 2019-nCoV and naming it SARS-CoV-2. *Nat. Microbiol.* 2020;5:536–544.
2. WHO. World Health Organization. WHO coronavirus disease (COVID-19) Dashboard [EB/OL]. https://covid19.who.int; 2022.
3. Yi Y, Zhang M, Xue H, et al. Schaftoside inhibits 3CL^{pro} and PL^{pro} of SARS-CoV-2 virus and regulates immune response and inflammation of host cells for the treatment of COVID-19. *Acta Pharm Sin B.* 2022;12:4154–4164.
4. Shen KY, Yang CH, Chen CT, et al. Omicron-specific mRNA vaccine induced cross-protective immunity against ancestral SARS-CoV-2 infection with low neutralizing antibodies. *J Med Virol.* 2023;95, e28370.
5. Khiali S, Khani E, Rouy SB, Entezari-Maleki T. Comprehensive review on molnupiravir in COVID-19: a novel promising antiviral to combat the pandemic. *Future Microbiol.* 2022;17:376–390.
6. Mannar D, Saville JW, Zhu X, et al. SARS-CoV-2 omicron variant: antibody evasion and cryo-EM structure of spike protein–ACE2 complex. *Science.* 2022;375:760–764.
7. Hirabara SM, Serdan TDA, Gorjao R, et al. SARS-COV-2 variants: differences and potential of immune evasion. *Front Cell Infect Microbiol.* 2022;11, 781429.
8. Huang FF, Li Y, Leung ELH, et al. A review of therapeutic agents and Chinese herbal medicines against SARS-COV-2 (COVID-19). *Pharmacol Res.* 2020;158, 104929.
9. Liu SY, Wang W, Ke JP, et al. Discovery of *Camellia sinensis* catechins as SARS-CoV-2 3CL protease inhibitors through molecular docking, intra and extra cellular assays. *Phytomedicine.* 2022;96, 153853.
10. Karges J, Giardini MA, Blacque O, et al. Enantioselective inhibition of the SARS-CoV-2 main protease with rhenium(i) picolinic acid complexes. *Chem Sci.* 2023;14:711–720.
11. Zhao J, Ma QH, Zhang BY, et al. Exploration of SARS-CoV-2 3CL^{pro} inhibitors by virtual screening methods, FRET detection, and CPE assay. *J Chem Inf Model.* 2021;61:5763–5773.
12. Newman DJ, Cragg GM. Natural products as sources of new drugs over the nearly four decades from 01/1981 to 09/2019. *J. Nat. Prod.* 2020;83:770–803.
13. Zhang DQ, Hamdoun S, Chen RH, et al. Identification of natural compounds as SARS-CoV-2 entry inhibitors by molecular docking-based virtual screening with bio-layer interferometry. *Pharmacol Res.* 2021;172, 105820.
14. Qiao LS, Huang WT, Zhang XL, et al. Evaluation of the Immunomodulatory effects of anti-COVID-19 TCM Formulae by multiple virus-related pathways. *Signal Transduct. Target. Ther.* 2021;6:50.
15. Yang ZH, Liu YX, Wang L, et al. Traditional Chinese medicine against COVID-19: role of the gut microbiota. *Biomed Pharmacother.* 2022;149, 112787.
16. Huang K, Zhang P, Zhang ZH, et al. Traditional Chinese Medicine (TCM) in the treatment of COVID-19 and other viral infections: Efficacies and mechanisms. *Pharmacol Therapeut.* 2021;225, 107843.
17. Luo L, Jiang JW, Wang C, et al. Analysis on herbal medicines utilized for treatment of COVID-19. *Acta Pharm Sin B.* 2020;10:1192–1204.
18. Yang K, Qiu J, Huang ZC, et al. A comprehensive review of ethnopharmacology, phytochemistry, pharmacology, and pharmacokinetics of *Schisandra chinensis* (Turcz.) Baill. and *Schisandra sphenanthera* Rehd. et Wils. *J Ethnopharmacol.* 2022;284, 114759.
19. Xiao WL, Huang SX, Wang RR, et al. Nortriterpenoids and lignans from *Schisandra sphenanthera*. *Phytochemistry.* 2008;69:2862–2866.
20. Liang CQ, Hu J, Luo RH, et al. Six new lignans from the leaves and stems of *Schisandra sphenanthera*. *Fitoterapia.* 2013;86:171–177.
21. Song QY, Zhang CJ, Li Y, et al. Lignans from the fruit of *Schisandra sphenanthera*, and their inhibition of HSV-2 and adenovirus. *Phytochem Lett.* 2013;6:174–178.
22. Zhou Z, Zhu CS, Zhang B. Study on medication regularity of traditional Chinese medicine in treatment of COVID-19 based on data mining. *Zhongguo Zhongyao Zazhi.* 2020;45:1248–1252.
23. Qi JH, Dong FX, Wang K, et al. Feasibility analysis and mechanism exploration of *Rhei Radix et Rhizome–Schisandrae Sphenantherae Fructus* (RS) against COVID-19. *J Med Microbiol.* 2022;71, 001528.
24. Ma CL, Sacco MD, Hurst B, et al. Boceprevir, GC-376, and calpain inhibitors II, XII inhibit SARS-CoV-2 viral replication by targeting the viral main protease. *Cell Res.* 2020;30:678–692.
25. Su HX, Yao S, Zhao WF, et al. Anti-SARS-CoV-2 activities *in vitro* of Shuanghuanglian preparations and bioactive ingredients. *Acta Pharmacol Sin.* 2020;41:1167–1177.
26. Yi Y, Li JH, Lai XY, et al. Natural triterpenoids from licorice potently inhibit SARS-CoV-2 infection. *J Adv Res.* 2022;36:201–210.
27. Nebigil CG, Moog C, Vagner S, et al. Flavaglines as natural products targeting eIF4A and prohibitins: from traditional Chinese medicine to antiviral activity against coronaviruses. *Eur J Med Chem.* 2020;203, 112653.
28. Li B, Xiao Q, Liu JS, et al. Chemical characterization and potential mechanism of the anti-asthmatic activity of a subfraction from *Schisandra chinensis* fruit extract. *J Agric Food Chem.* 2022;70:5015–5025.
29. Jiang H, Chen J, Li X, et al. Systematic identification of chemical components in Fufang Shuanghua oral liquid and screening of potential active components against SARS-CoV-2 protease. *J Pharm Biomed Anal.* 2023;223, 115118.
30. Muralidharan N, Sakthivel R, Velmurugan D, Gromiha MM. Computational studies of drug repurposing and synergism of lopinavir, oseltamivir and ritonavir binding with SARS-CoV-2 protease against COVID-19. *J Biomol Struct Dyn.* 2021;39:2673–2678.
31. Dubuc I, Prunier J, Lacasse É, et al. Cytokines and lipid mediators of inflammation in lungs of SARS-CoV-2 infected mice. *Front Immunol.* 2022;13, 893792.
32. Zhu JJ, Zhang HY, Lin QH, et al. Progress on SARS-CoV-2 3CL^{pro} inhibitors: inspiration from SARS-CoV 3CL^{pro} peptidomimetics and small-molecule anti-inflammatory compounds. *Drug Des. Devel. Ther.* 2022;16:1067–1082.
33. Nasonov E, Samsonov M. The role of interleukin 6 inhibitors in therapy of severe COVID-19. *Biomed Pharmacother.* 2020;131, 110698.
34. Andreakos E, Papadaki M, Serhan CN. Dexamethasone, pro-resolving lipid mediators and resolution of inflammation in COVID-19. *Allergy.* 2021;76:626–628.
35. Sharma VK, Prateeksha, Singh SP, et al. Nanocurcumin potently inhibits SARS-CoV-2 spike protein-induced cytokine storm by deactivation of MAPK/NF-κB signaling in epithelial cells. *ACS Appl Bio Mater.* 2022;5:483–491.
36. Cao W, Li TS. COVID-19: towards understanding of pathogenesis. *Cell Res.* 2020;30:367–369.